This is a repository copy of *Bio-inspired multi-agent model and optimization strategy for collaborative aerial transport*.

White Rose Research Online URL for this paper:
https://eprints.whiterose.ac.uk/176758/

Version: Accepted Version

This is a post-peer-review, pre-copyedit version of an article published in Deng Z. (eds) Proceedings of 2021 Chinese Intelligent Automation Conference. Lecture Notes in Electrical Engineering, vol 801. The final authenticated version is available online at: http://dx.doi.org/10.1007/978-981-16-6372-7_64.

Bio-inspired Multi-agent Model and Optimization Strategy for Collaborative Aerial Transport

Kangyao Huang[1], Jingyu Chen[2], John Oyekan, and Xinyu Zhang

[1] Tsinghua University, Beijing 100084, China,
kangyao.huang@outlook.com
[2] Department of Automatic Control and Systems Engineering, The University of
Sheffield, Mappin Street, Sheffield, S1 3JD,
jchen118@sheffield.ac.uk

Abstract. Collaboration between robots provides solutions for transporting more complex and heavier loads. In this work, inspired by the ant colony foraging and transport, we put forward two collaborative models, Coupled-Carriers and Navigator-Carrier, for aerial cooperative transport. To achieve this, a linear quadratic regulator (LQR) is applied to optimize the performance. The results show the task of dual-drone transport of a bar load is successfully accomplished.

Keywords: cooperative transport, swarm intelligence, swarm robotics, multi-agent system, optimal control

1 Introduction

In the last few years, UAVs(Unmanned Aerial Vehicles) are tested to deliver parcels to customers, which successfully shows huge advantages in solving problems in smart logistics. Besides, the swarm robotics system with reconfigurability, robustness, fault tolerance and flexibility has significant potential, and can be deployed in the cooperative framework [1]. Thus, it is undoubted that multi-agent cooperation technology is an imminent opportunity and challenge for the next generation of smart logistics.

Bio-inspired methodologies usually lead to satisfactory results in practical application in robotics. In [2], authors reveal the microscopic rules employed by individual ants and how their behaviours lead to the emergence of collective motion. In the coupled transport model, ants act as lifters and pullers led by informed ants which know the destination. To complete the cooperative transport efficiently, ants in the swarm need to maintain the direction of the nest independently if they know the goal. Besides, explicit communications for exchanging message for orientation correction and velocity alignment are also required in the team [3]. The opposite also exists that parts of agents do not need to acquire the direction, alignment can be carried out by tracking other carriers' actions. The collective foraging behaviour of the ant colony shows a great value to swarm

robotics cooperative transportation providing a significant inspiration, which provides a convincing motivation.

In this work, cable suspended is chosen as the transport method due to its flexibility for the team formation control. The most related work to the coupled-carriers model is [4]. In [5], the authors present a linear quadratic regulator (LQR) controller for maintaining the stability of lifting and transporting a payload by a flexible cable. However, they evaluate the only single-drone system and we focus on the dual-drone system. The contributions of this work include mainly three points:

1. The dynamic model of the dual-drone cooperative transport system with LQR is established and evaluated, to optimize the tracking performance between the carrier and the load.
2. Two collaborative transport models are proposed which are inspired by roles and behavioural transitions in ant colony foraging.

2   Methodology

Agents and their characters in the collaborative work is assumed to have the following properties: (1) Carriers are not aware of the environment, but have local positioning ability that can flock; (2) Navigators or coupled-carriers have complete prior knowledge about the global environment; (3) Carriers can only provide the lifting force, navigators can only provide the navigation, and coupled-carriers can provide both abilities described above.

2.1   Flocking Behaviour

The flocking behaviour controller is based on Reynolds rules [6]: separation for obstacle avoidance, cohesion for staying close to the flocking centre, and friction for matching velocities of neighbouring members. Also, this controller utilizes relative position $\boldsymbol{p_i}$ for its neighbour i.

Velocity control is employed for fulfilling the velocity constraints of the flocking controller at a constant height, which can be concluded as (1)

$$\boldsymbol{v}_n^f = \boldsymbol{v}_n^{sep} + \boldsymbol{v}_n^{coh} + \boldsymbol{v}_n^{frict} \tag{1}$$

where $\boldsymbol{v}_n^{sep}, \boldsymbol{v}_n^{coh}, \boldsymbol{v}_n^{frict}$ relate to the corresponding Reynolds velocity components, which can be described as

$$
\begin{aligned}
\boldsymbol{v}_n^{sep} &= -\frac{k_{sep}}{\mathbb{N}} \sum_{i \in \mathbb{N}} \frac{\boldsymbol{p}_i}{\|\boldsymbol{p}_i\|^2} \\
\boldsymbol{v}_n^{coh} &= \frac{k_{coh}}{\mathbb{N}} \sum_{i \in \mathbb{N}} \frac{\boldsymbol{p}_i}{\|\boldsymbol{p}_i\|^2}
\end{aligned}
\tag{2}
$$

where k_{sep} and k_{coh} are predefined constant separation and cohesion gains, and $\mathbb{N}$ denotes now many neighbours surrounding the n th agent. The friction

regulation depresses the vibrations of robots along the flocking velocity intending to reach a steady state expeditiously. The relative velocity of the ith neighbour is indicated as $\dot{\boldsymbol{p}}_i$ $w.r.t$ the body reference system of the current robot. Thus, friction velocity is

$$\boldsymbol{v}_n^{frict} = \frac{k_{frict}}{\mathbb{N}} \sum_{i \in \mathbb{N}} \dot{\boldsymbol{p}}_i \tag{3}$$

where k_{frict} is friction gains that influence the intensity of the inhibitory effect, and the relative velocity $\dot{\boldsymbol{p}}_i$ is obtained by the differential of $\boldsymbol{p}_i$.

2.2 Coupled-Carriers Model and Optimization Strategy

The coupled-carriers model adopts a leader-follower scheme built by two drones attached to a rod-shaped load.

The centre mass points of UAVs are connected to two sides of the load using cables. To enhance the robustness of the system and eliminate the oscillation, we draw on the experience of [4] and solve the dual lift problem by decomposing it into decoupled systems. The leader drone controlled by a linear quadratic regulator (LQR) is responsible for controlling the load position (x, y, z). The follower tracks the leader by the landmark and adjusts its heading to align the leader's direction, then shares half of the payload mass by keeping equal space with the leader. The system overview is shown in Fig.1.

(a) Leader-follower system   (b) slung load system
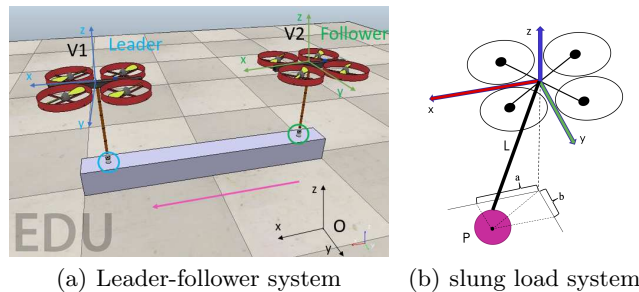
Fig. 1: The leader-follower system for cooperative transportation. The leader (left) controls the 3D position of the payload connection point. The follower (right) follows the transportation direction; a and b are the relative pendulum position along x and y axis respectively.

The transport system is similar to the previous work of the inverted pendulum in [7, 8] but we assume the payload is underneath the quadrotor instead. As is shown in Fig.1b, the base of the pendulum is attached to the mass centre of a drone. And the tip of the pendulum is assumed to be the mass centre of the payload (ignoring the mass of the pendulum). The translation position q of the drone is measured in the inertial coordinate. For the pendulum, its position p is defined relative to the base of the pendulum in the x and y axis respectively.

The nonlinear motion equation of the quadrotor-pendulum system can be concluded as:

$$\dot{x} = g(x, u) \tag{4}$$

and $x = [q \quad p \quad \dot{q} \quad \dot{p}]^T = [x \quad y \quad z \quad a \quad b \quad \dot{x} \quad \dot{y} \quad \dot{z} \quad \dot{a} \quad \dot{b}],$

$$u = [\phi \quad \theta \quad T]$$

where $[\phi \quad \theta \quad T]$ shows the roll, pitch, and the thrust of the drone.

The linear quadratic regulator (LQR) is introduced to cancel out the deviation from the desired states x_{des} of the quadrotor and pendulum, trying to eliminate the oscillation of the load and optimize the transport performance. For the motion equation (4), we find some states contain the nonlinear part, and thus linearization of the equation is required. We apply first *Taylor* approximation to (4) around the desired states x_{des} and the desired input u_{des} especially for $\ddot{a}$ and $\ddot{b}$:

$$g(a, b, \dot{a}, \dot{b}, \phi, \theta, T) = g(a_{des}, b_{des}, \dot{a}_{des}, \dot{b}_{des}, \phi_{des}, \theta_{des}, T_{des})$$

$$+ \left.\frac{\partial g}{\partial a}\right|_{x_{des}, u_{des}} (a - a_{des}) + \left.\frac{\partial g}{\partial b}\right|_{x_{des}, u_{des}} (b - b_{des}) + \left.\frac{\partial g}{\partial \dot{a}}\right|_{x_{des}, u_{des}} (\dot{a} - \dot{a}_{des})$$

$$+ \left.\frac{\partial g}{\partial \phi}\right|_{x_{des}, u_{des}} (\phi - \phi_{des}) + \left.\frac{\partial g}{\partial \theta}\right|_{x_{des}, u_{des}} (\theta - \theta_{des}) + \left.\frac{\partial g}{\partial T}\right|_{x_{des}, u_{des}} (T - T_{des}) \tag{5}$$

This linearization relates to the multi-variate Taylor approximation. After that, we obtain the new discrete state equations with deviations,

$$\tilde{x}_{(k+1)} = A_d \tilde{x}_{(k)} + B_d \tilde{u}_{(k)} \tag{6}$$

To compute the state feedback control gain K of the LQR controller, we design penalty matrices Q and R for the system shown as

$$K = lqrd(A, B, Q, R)$$

Thus, the optimal feedback control $\tilde{u}_k = -K\tilde{x}_k$ is achieved by minimizing the cost function J,

$$J = \sum_{k=0}^{\infty} \tilde{X}_k^T Q \tilde{X}_k + \tilde{U}_k^T R \tilde{U}_k$$

2.3   Navigator-Carriers Model

Based on the coupled-carriers model, the navigator-carrier architecture is established by decoupling the functions of coupled-carrier, shown in Fig.2. The navigators give up the lifting ability and concentrate on navigation tasks.

Compared with the coupled-carrier model, this strategy has significant advantages in that the navigators will not be restricted by the swarm. They are not required to be linked with the load and have more freedom to search the environment thoroughly. In practice, agents rarely have a clear understanding of their surroundings. Therefore, navigators should frequently leave the swarm to map the whole environment to get a better cognition of unknown circumstance.
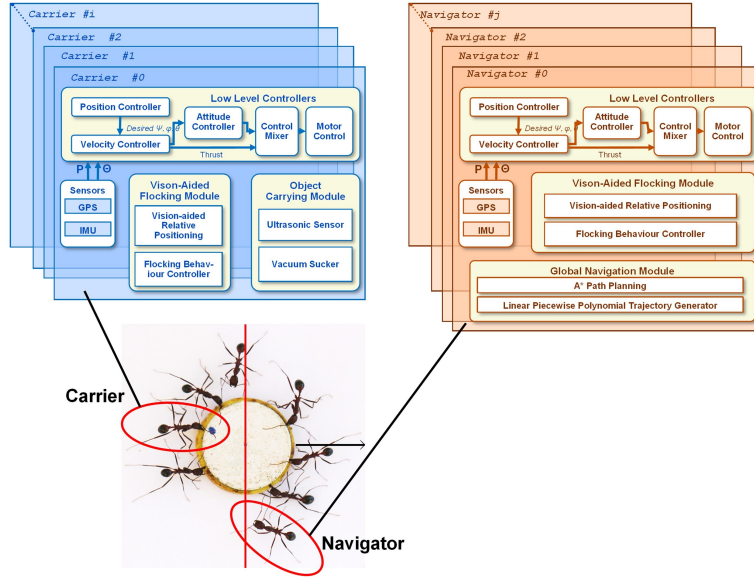
Fig. 2: Navigator-carriers Model

3   Experimental Results and Discussion

Two experiments are designed in this part: coupled-carriers and navigator-carrier transport experiment. The simulation runs in the robot simulator *CoppeliaSim*. In simulator, the drone weighs 520g meanwhile it can lift up to 80g payload, and the size is $0.3 \times 0.3 \times 0.2m$. For the suspended system, the mass of rope and vacuum sucker is about 36g, and the cable length is about 0.5m. The load size is $0.4 \times 0.4 \times 1.0m$, and the weight is about 120g.

3.1   Coupled-Carriers Cooperative Transport

In this experiment, we generate a linear piece-wise polynomial tracking trajectory of a 3.3m straight line with the maximum velocity of 1 m/s for the leader connection point of the load at a constant height.

The results are obtained from the experiment of straight-line transport by two drones. In the predefined 3.3-metre polynomial trajectory, the leading UAV is accelerating to the maximum speed of 1 m/s and then decelerating. Finally, the payload is carried to the destination and hovers right above the conveyor belt. The whole trajectories of drones are captured in Fig.3.

To investigate the performance of the following capability, real positions, tracking errors, and velocities between the leader and follower, are plotted in Fig.4, which shows the effectiveness of the Coupled-Carriers model.
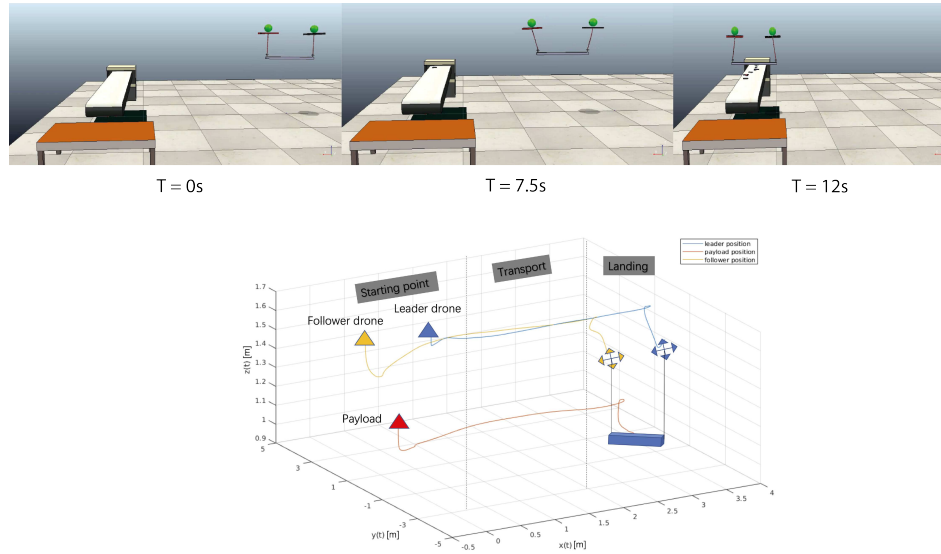
Fig. 3: Snapshots and trajectories for cable-suspended cooperative transport by two UAVs

3.2   Navigator-Carrier Collaborative Transport

To verify the effect of navigator-carrier collaborative transport, three drones are used and transport a stick cargo from the initial point.

These results show how the navigator-carrier model collaboratively transport an object. The snapshots and trajectories of all entities of this collaborative transport are shown in Fig. 5 which proves the effectiveness of the navigator-carrier model.

4   Conclusion

This work mainly studies a bio-inspired model acquired from ant colony foraging and introduces two models for collaborative transport. Both of these models can achieve collaborative tasks successfully. The LQR controller is applied in a slung-payload system to track the predefined trajectories during the transport where smooth trajectories and good stability have been shown in the coupled-carriers scene.

References

1. Chung, S.J., Paranjape, A.A., Dames, P., Shen, S., Kumar, V.: A Survey on Aerial Swarm Robotics. IEEE Transactions on Robotics **34**(4), 837–855 (2018). DOI 10.1109/TRO.2018.2857475
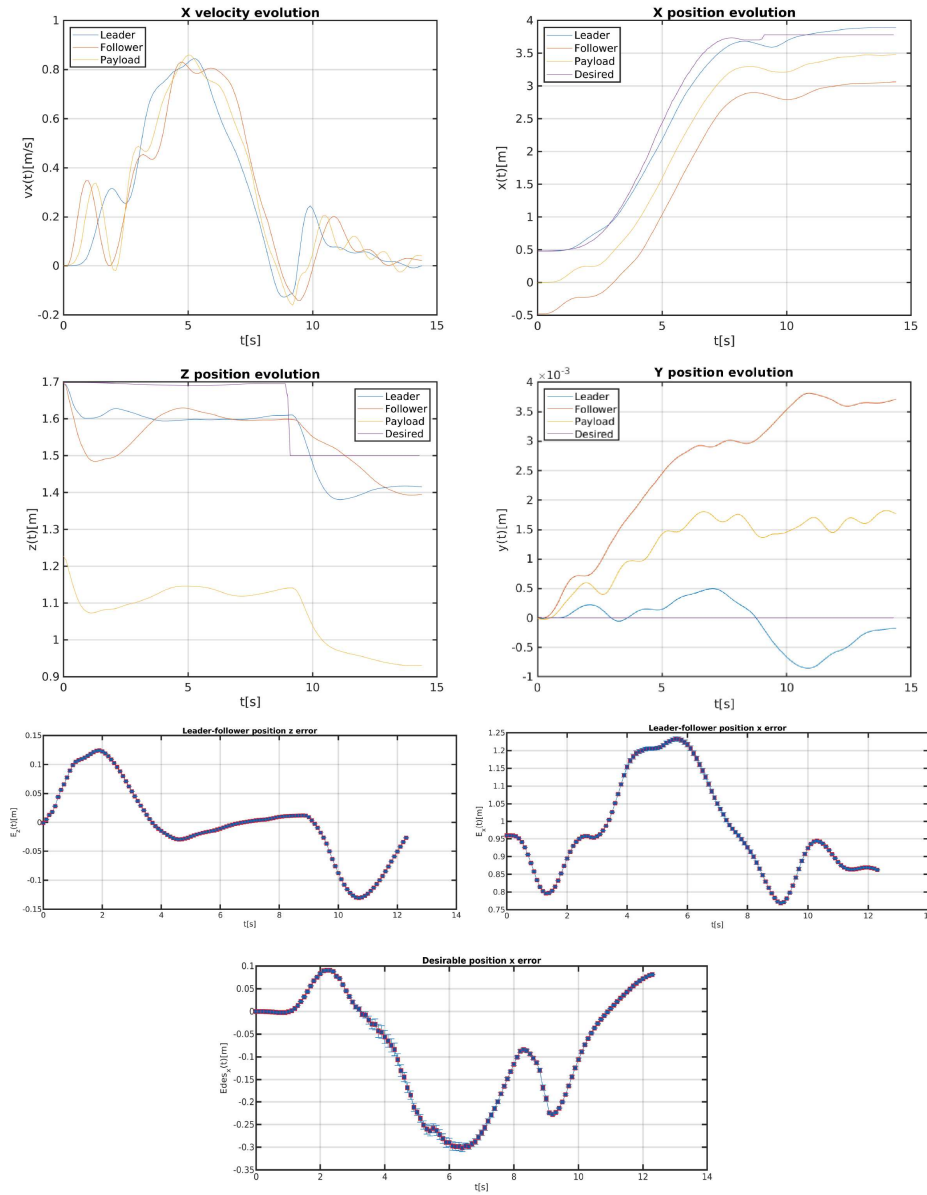
Fig. 4: Data record during the transport: x velocity evolution records the velocity changes of entities along the path; x, y, z position evolution respectively record the position tracking performance; the tracking error between leader and follower is recorded in Leader-follower position x, z error, and the last graph records the real error between the leader and desired path. The error bar graphs use data of 5 successful runs by calculating the average and variance
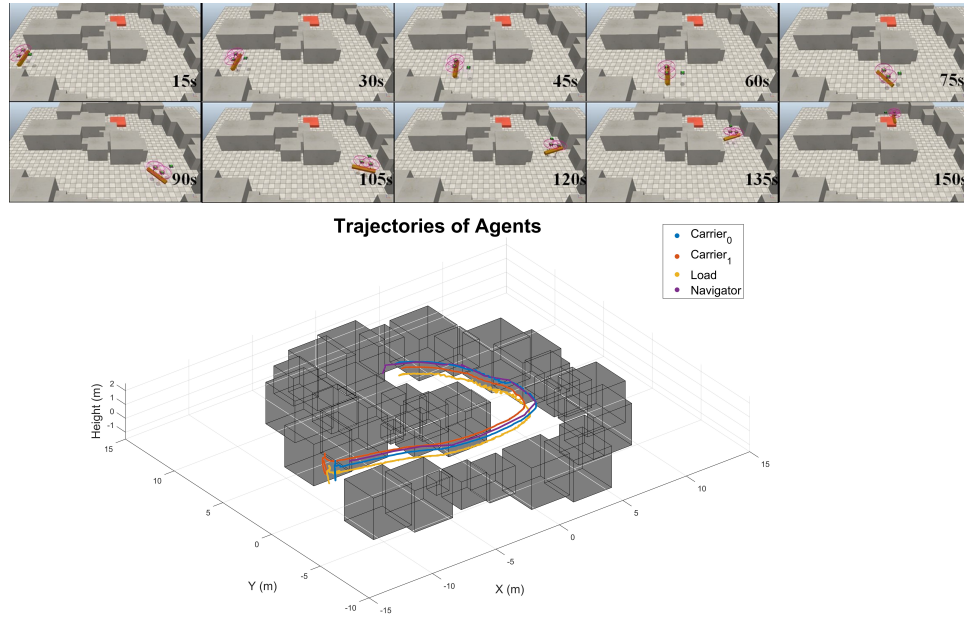
Fig. 5: Navigator-carrier model transport snapshots and trajectories.

2. Feinerman, O., Pinkoviezky, I., Gelblum, A., Fonio, E., Gov, N.S.: The physics of cooperative transport in groups of ants. Nature Physics **14**(7), 683–693 (2018). DOI 10.1038/s41567-018-0107-y

3. Czaczkes, T.J., Ratnieks, F.L.: Cooperative transport in ants (Hymenoptera: Formicidae) and elsewhere. Myrmecological News **18**, 1–11 (2013)

4. Gassner, M., Cieslewski, T., Scaramuzza, D.: Dynamic collaboration without communication: Vision-based cable-suspended load transport with two quadrotors. Proceedings - IEEE International Conference on Robotics and Automation pp. 5196–5202 (2017). DOI 10.1109/ICRA.2017.7989609

5. Alothman, Y., Jasim, W., Gu, D.: Quad-rotor lifting-transporting cable-suspended payloads control. 2015 21st International Conference on Automation and Computing: Automation, Computing and Manufacturing for New Economic Growth, ICAC 2015 (2015). DOI 10.1109/IConAC.2015.7313996

6. Reynolds, C.W.: Flocks, Herds, and Schools: A Distributed Behavioral Model **21**(July), 25–34 (1987)

7. Hehn, M., D'Andrea, R.: A flying inverted pendu lum. Proceedings - IEEE International Conference on Robotics and Automation (2), 763–770 (2011). DOI 10.1109/ICRA.2011.5980244

8. Maughan, D.S., Erekson, I.T., Sharma, R.: Flying inverted pendulum trajectory control on Robust Intelligent Sensing and Control Multi-Agent Analysis Platform. 2015 International Conference on Unmanned Aircraft Systems, ICUAS 2015 (July), 1279–1284 (2015). DOI 10.1109/ICUAS.2015.7152421